Eur Biophys J (2000) 28: 629–638

ARTICLE

Patrick Garidel · Alfred Blume

Miscibility of phosphatidylethanolamine-phosphatidylglycerol mixtures as a function of pH and acyl chain length

Received: 3 August 1998 / Revised version: 4 October 1999 / Accepted: 12 October 1999

Abstract We have examined the mixing properties of phosphatidylethanolamine (PE) and phosphatidylglycerol (PG), the major components of many bacterial membranes. The phase transition behavior of dilute aqueous suspensions of PE:PG mixtures with different chain lengths (n = 14, 16) in 0.1 M NaCl at pH 7 and pH 2 was investigated by differential scanning calorimetry (DSC). The DSC curves were simulated using an approach which takes into account the broadening of the phase transition in addition to symmetric, non-ideal mixing in the gel and the liquid-crystalline phase. Based on the temperatures for onset and end of "melting" obtained by the simulations, the phase diagrams were constructed and then refined using a regular solution model with non-symmetric mixing in both phases. The mixing properties of PE:PG mixtures were analyzed as a function of pH and acyl chain length. In almost all cases, non-symmetric mixing behavior was observed, i.e. the non-ideality parameters are different for bilayers with low PG content compared to bilayers with high PG content. For equimolar mixtures at pH 7, when PG is negatively charged, the non-ideality parameters are negative for both phases, indicating preferential formation of mixed pairs. This mixed pair formation is more pronounced for the gel phase. At pH 2, when PG is partly protonated, the non-ideality parameter is less negative and the formation of mixed pairs is reduced compared to pH 7. The formation of PE:PG mixed pairs at pH 7 might be of benefit to a bacterial membrane, because it prevents demixing of lipid components with a concomitant destabilization of the membrane.

Key words Phosphatidylethanolamine · Phosphatidylglycerol · Differential scanning calorimetry · Phase diagrams · Non-ideality parameter

P. Garidel · A. Blume (✉)
Martin-Luther-Universität Halle-Wittenberg,
Institute of Physical Chemistry, Mühlpforte 1,
D-06108 Halle/Saale, Germany
e-mail: blume@chemie.uni-halle.de

Introduction

From a biophysical and biotechnological point of view, the relationship between structure and function of biomembranes is a subject of great interest. The physical and functional properties of biomembranes depend on the arrangement and the distribution of the membrane components within the bilayer (MacFarlane 1964; Cronan and Gelman 1975; Jacobson and Papahadjopoulos 1975; Metcalf et al. 1986; Tocanne et al. 1994; Heimburg and Marsh 1996). In particular, variations in the chemical structures of the lipids resulting in different lateral distribution of membrane components are of fundamental importance for biomembrane functions.

Phosphatidylcholines (PCs) and phosphatidylethanolamines (PEs) are abundant phospholipids in biological membranes. Pseudobinary phospholipid mixtures of PCs and PEs with other phospholipids (zwitterionic or negatively charged) have therefore been studied extensively in recent years. However, a systematic study of PE-phosphatidylglycerol (PG) mixtures has not been performed despite the fact that many membranes of bacteria contain these two lipids in large quantities. For instance, in the membrane of *Escherichia coli*, the main lipid fractions are PE with ≈80 wt% and PG with 10–15% of the total lipid pool (Cronan and Vagelos 1972; Gally et al. 1980; Borle and Seelig 1985).

To obtain more insight into the organization of these two phospholipid classes in a bilayer, we have investigated by differential scanning calorimetry (DSC) the mixing behavior of PG with PE as a function of acyl chain length and degree of protonation. These studies were also performed with respect to the question of domain formation in lipid membranes, which has attracted increasing attention in the past years (Bloom et al. 1991; Vaz 1994, 1995; Welti and Glaser 1994; Yang and Glaser 1996; Denisov et al. 1998).

We have employed a method to determine more objectively the temperatures for onset and end of melting from the DSC thermograms by fitting the experimental

heat capacity curves using one non-ideality parameter for each phase and an additional parameter which takes into account the broadening of the C_p curves. These simulations showed that the non-ideality parameters are a function of composition. From the temperatures of beginning and end of "melting", phase diagrams were constructed and then refined using two non-ideality parameters for each of the phases to account for non-ideal and non-symmetric mixing. The exact simulation procedure with its limitations has been described before (Mennicke 1995; Johann et al. 1996; Garidel et al. 1997a).

The following pseudobinary systems (in 0.1 M NaCl) were investigated at two different pH values, namely pH 7 and pH 2: DMPG:DMPE, DPPE:DPPG, DMPE:DPPG, and DPPE:DMPG. The experiments showed that, in PE:PG mixtures, complex formation of unlike molecules can occur in the gel phase and also in the liquid-crystalline state. Protonation of the PG headgroup leads to changes in the mixing behavior, reducing the preferential formation of mixed pairs.

Materials and methods

1,2-Dipalmitoyl-*sn*-glycero-3-phosphoethanolamine (DPPE), 1,2-dimyristoyl-*sn*-glycero-3-phosphoethanolamine (DMPE), 1,2-dipalmitoyl-*sn*-glycero-3-phosphoglycerol (DPPG, Na salt), and 1,2-dimyristoyl-*sn*-glycero-3-phosphoglycerol (DMPG, Na salt) were obtained from Nattermann Phospholipid (Cologne, Germany), Sygena (Liestal, Switzerland), and Lipoid (Ludwigshafen, Germany). The lipid purity was checked by thin layer chromatography (TLC).

The preparation of the samples was performed in the following way. Binary lipid mixtures were prepared from lipid stock solutions in chloroform/methanol (2:1, v/v) as solvent by mixing appropriate volumes of the stock solutions. The organic solvent was then rapidly removed in a stream of argon at elevated temperature. The resulting lipid films were kept in an evacuated flask for 24 h to remove residual traces of solvent. The aqueous dispersions were then prepared by adding a certain volume of an aqueous 0.1 M NaCl solution to obtain a total lipid concentration of 2.5 mg/ml. The samples were vigorously vortexed for 5 min at 75–80 °C and then for a further 5 min a room temperature to obtain a homogeneous suspension. The pH of the samples was checked and adjusted by addition of HCl or NaOH, respectively, before the vortexing procedure. If necessary, this procedure was repeated. The preparation procedure leads to large multilamellar liposomes.

The DSC measurements were performed with a MicroCal MC-2 scanning calorimeter (MicroCal, Northampton, Mass., USA). The heating rate was 1 °C/min. Three scans were performed to check for reproducibility of the DSC curves. The purity of the samples was checked before and after the scans using TLC. For samples at pH 2, only the first two scans were used because of detectable hydrolysis products.

Three individually prepared samples were measured to test the reproducibility of the sample preparation. The accuracy of the DSC experiments was ± 0.1 °C for the main phase transition temperature T_m and ± 0.2 kcal/mol for the main phase transition enthalpy ΔH_{cal}.

The methods used for the simulation of the heat capacity curves and the fitting of the phase diagrams have been described before (Johann et al. 1996; Garidel et al. 1997a, b). The applied model for the simulation of the phase diagrams is based on regular solution theory using non-ideal, non-symmetric mixing for both phases, the liquid-crystalline as well as the gel phase. The excess Gibbs free energy of mixing, ΔG^E, is given as $\Delta G^E = x(1-x)[\rho_1 + \rho_2(2x-1)]$, with x being the mole fraction of the second component. Therefore, two non-ideality parameters, ρ_1 and ρ_2, are obtained for both phases, the first one describing the non-ideality at $x = 0.5$, the second one the asymmetry. The non-ideality parameters describe the deviation from ideal mixing, positive values indicate demixing, negative a tendency for mixed pair formation.

Results

PEs and PGs in excess water

At pH 7 (0.1 M NaCl), PGs are negatively charged and PEs are zwitterionic. At pH 2, the phosphodiester group of PGs ($pK_a \sim 2.9$) is mainly protonated (≈90%) (Garidel et al. 1997b). In Table 1 we have summarized the thermodynamic data of the pure phospholipid components at pH 7 and pH 2 in 0.1 M NaCl. These data (T_m and ΔH_m) were used as input parameters for the simulation of the C_p curves and phase diagrams. The data for the pretransition of the PGs were reported in our previous paper (Garidel et al. 1997b). Our results are in good agreement with previously published data (Jacobson and Papahadjopoulos 1975; Träuble 1976; Träuble et al. 1976; Cevc et al. 1980; Blume 1988, 1991).

The effect of changing the pH to 2 on the phase transition temperature T_m of PEs is very small. T_m of

Table 1 Thermodynamic data for the main phase transition of phospholipids in 0.1 M NaCl. T_m = maximum of the C_p curve, $T_{1/2}$ = half width of the transition, ΔH_{cal} = calorimetrically determined transition enthalpy

Lipid	pH 2			pH 7		
	T_m (°C)	$T_{1/2}$ (°C)	ΔH_{cal} (kcal mol^{-1})	T_m (°C)	$T_{1/2}$ (°C)	ΔH_{cal} (kcal mol^{-1})
DMPE	49.6	2.3	5.0	48.8	1.8	4.9
DMPG	41.4	2.0	6.7	23.3	0.7	7.4
DPPE	64.5	2.3	10.6	63.4	1.3	9.2
DPPG	58.3	3.5	9.2	40.0	0.9	8.2

PEs increases by only 1 °C (Träuble and Eibl 1974; Boggs 1987; Cevc 1990) and the transition enthalpy (L_β to L_α) changes by not more than 1 kcal/mol (see Table 1). The pK of the phosphodiester group in PEs has been reported to be 1.9 (Tatulian 1992) or even lower (pK = 0.32) (Standish and Pethica 1968). Our DSC experiments indicate that the apparent pK under our experimental conditions is probably well below 1.9, i.e. even at pH 2 the headgroup of PEs is still mainly zwitterionic, with only 5–10% of the headgroups being protonated.

PE:PG mixtures in excess water

Figures 1–4 show the third (pH 7) and the first (pH 2) heating scans (see Garidel et al. 1997b) obtained for the four PE:PG systems dispersed in 0.1 M NaCl. On the left side of Figs. 1–4 the molar ratio of both components are listed. The solid lines represent the experimentally measured C_p curves and the dotted lines the simulated heat capacity curves C_p^{sim} obtained by the procedure described before (Johann et al. 1996).

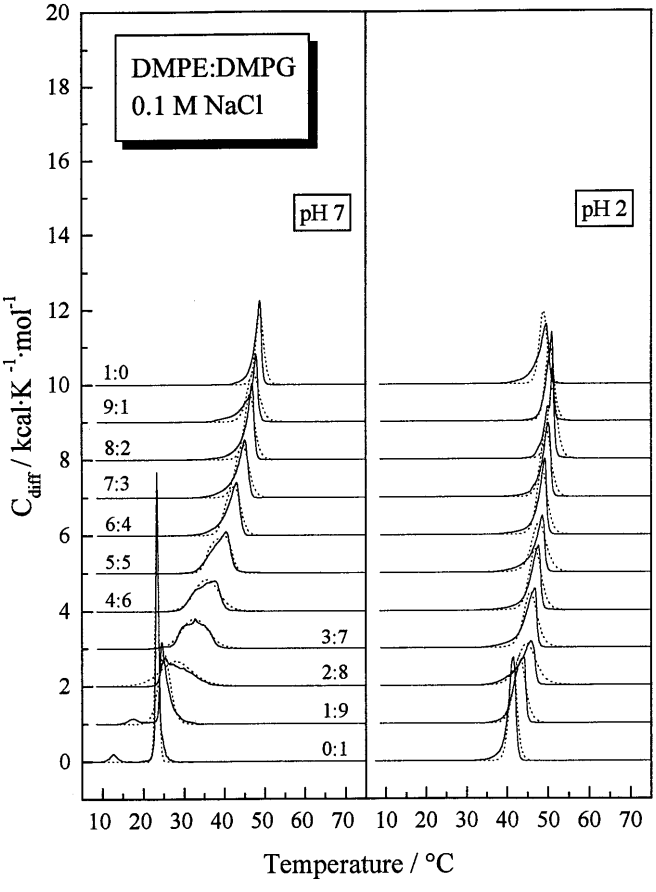

Fig. 1 DSC heating thermograms for the system DMPE:DMPG at various molar ratios at pH 7 and pH 2: experimental C_p curves (*solid line*) and simulated C_p curves (*dotted line*)

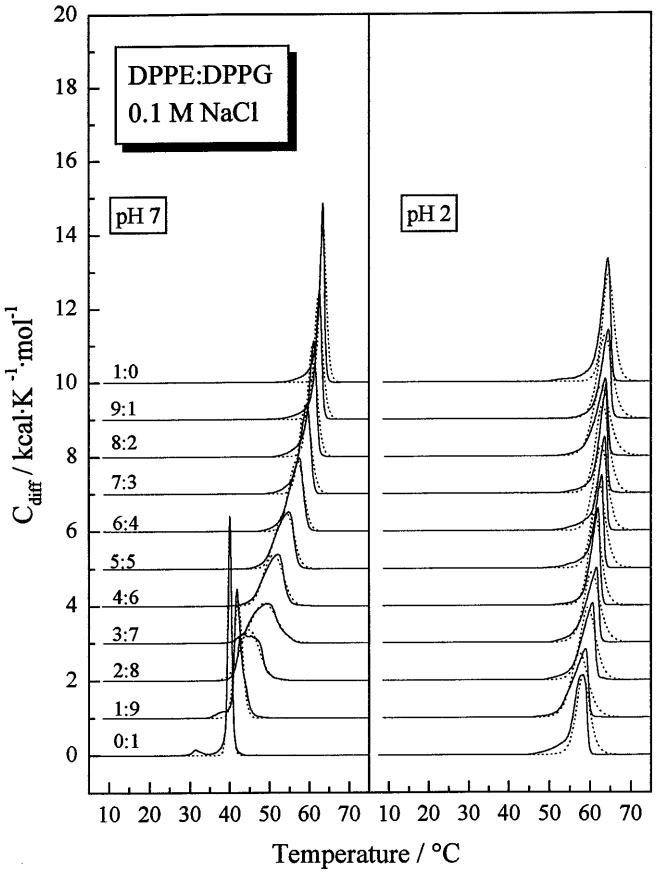

Fig. 2 DSC heating thermograms for the system DPPE:DPPG at various molar ratios at pH 7 and pH 2: experimental C_p curves (*solid line*) and simulated C_p curves (*dotted line*)

In the case of DPPE:DMPG mixtures at pH 7, where apparently a miscibility gap in the gel phase is observed (see Fig. 4), the simulation fails because the model is not suited to simulate C_p curves for phase diagrams with eutectic points. Therefore, for this particular mixture we have used the usual empirical procedure to determine the temperatures of the coexistence lines.

The temperatures $T(-)$ and $T(+)$ for the beginning and end temperatures of the phase transition are shown in Figs. 5–8. Based on these temperature data, the phase diagrams were refined using a model with non-ideal, non-symmetric mixing which we have described in previous papers (Johann et al. 1996; Garidel et al. 1997a, b). For comparison, the empirical temperatures $T^{\mathrm{exp}}(-)$ and $T^{\mathrm{exp}}(+)$ obtained in the usual way from the deviation of the experimental DSC curves from the baseline (Mabrey and Sturtevant 1976; Silvius and Gagné 1984a, b) are also shown as open $[T^{\mathrm{exp}}(-)]$ and as solid circles $[T^{\mathrm{exp}}(+)]$. The non-ideality parameters and the differences in the non-ideality parameters between the liquid-crystalline and gel states, $\Delta\rho_1 = \rho_{l1} - \rho_{g1}$ and $\Delta\rho_2 = \rho_{l2} - \rho_{g2}$ (index l for the liquid-crystalline phase and index g for the gel phase), obtained by the simulation of the phase diagrams are also included.

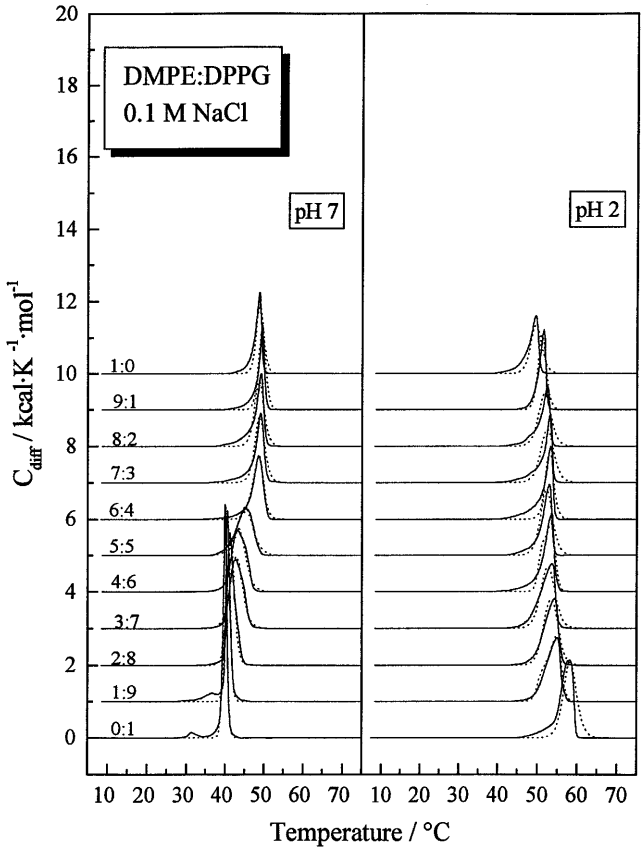

Fig. 3 DSC heating thermograms for the system DMPE:DPPG at various molar ratios at pH 7 and pH 2: experimental C_p curves (*solid line*) and simulated C_p curves (*dotted line*)

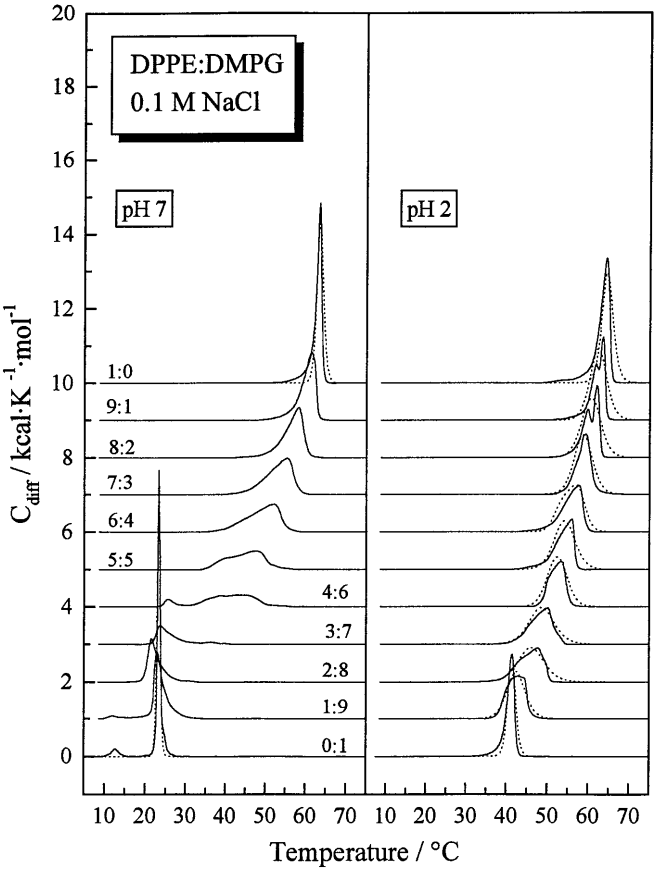

Fig. 4 DSC heating thermograms for the system DPPE:DMPG at various molar ratios at pH 7 and pH 2: experimental C_p curves (*solid line*) and simulated C_p curves (*dotted line*)

At pH 7, the pretransition vanishes in all mixtures with more than 10 mol% of the PE component. In mixtures with less than 10 mol% PE, a three-phase coexistence between the liquid-crystalline and two different gel phases has to be expected. However, the larger part of the phase diagram ($x_{PE} > 0.1$) is not influenced by this effect. Therefore, we used the simplified approach of assuming only one gel and one liquid-crystalline phase (see Garidel et al. 1997a, b).

The difference in non-ideality parameters between liquid-crystalline and gel phase, $\Delta\rho_c$, can be calculated using the non-ideality parameters obtained from the simulation of the whole phase diagram (data included in the Figs. 5–8) according to $\Delta\rho_c = \Delta\rho_1 + \Delta\rho_2(2x_{PG} - 1)$, with x_{PG} the mole fraction of the PG component and $\Delta\rho_1$ and $\Delta\rho_2$ the differences between the non-ideality parameters ρ_1 and ρ_2. These results are shown in Fig. 9.

DMPE:DMPG and DPPE:DPPG

pH 7. The heat capacity curves of these mixtures are shown on the left hand side in Figs. 1 and 2. With increasing amounts of the higher melting component (DMPE or DPPG, respectively) an increase of the phase transition temperature is observed as expected, and the pretransition disappears above 10 mol% PE. The phase diagrams of DMPE:DMPG and DPPE:DPPG mixtures at pH 7 (Figs. 5 and 6) show a broad coexistence range due to the difference in transition temperature of the two components. The T_m difference is 25.5 °C in the first case and 23.4 °C in the latter. The non-ideality parameters ρ_1 obtained from the simulation of the phase diagram are all negative with $\rho_{g1} < \rho_{l1}$, which leads to a positive $\Delta\rho_1$. The difference of the asymmetry term $\Delta\rho_2$ is −220 to −250 cal/mol ($\rho_{g2} > \rho_{l2}$) (see Table 2).

pH 2. Partial protonation of DMPG or DPPG shifts its transition temperature upwards by approximately 18 °C. The difference in T_m of PGs and PEs is now reduced to 6–8 °C. Consequently, the coexistence range in DMPE:DMPG and DPPE:DPPG mixtures at pH 2 (right hand side of Figs. 1 and 2) is narrower and the non-ideality parameters obtained from the simulation of the phase diagram are reduced compared to the systems at pH 7. The exact calculation of the non-ideality parameters becomes difficult for these mixtures, the absolute values having large errors. The differences in non-ideality parameters are more reliable as mentioned before (Johann et al. 1996). The gel phase $\rho_{g1,2}$ parameters are

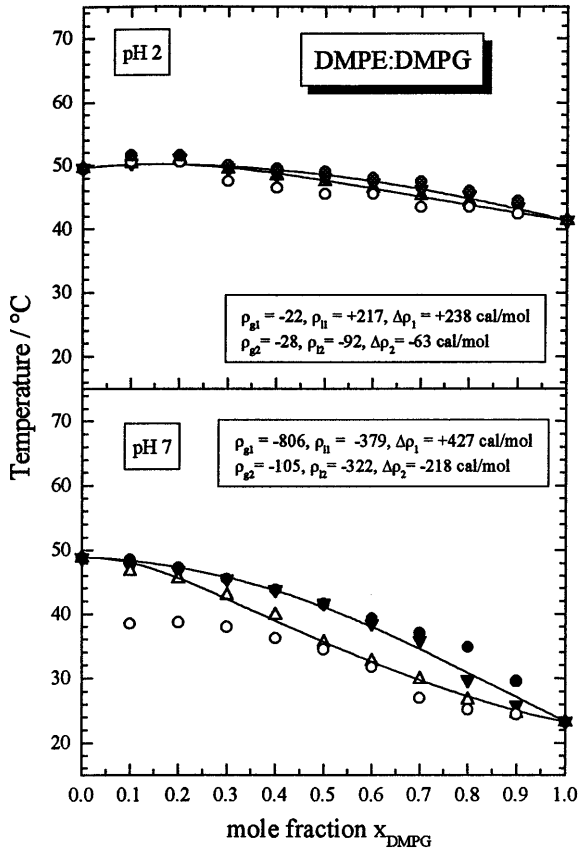

Fig. 5 Pseudobinary phase diagrams for the system DMPE:DMPG at pH 2 and pH 7. *Triangles* are $T(-)$ and $T(+)$ values obtained from the simulation of the C_p curve; *circles* are $T^{exp}(-)$ and $T^{exp}(+)$ values obtained by the usual empirical procedure. The *solid lines* are the coexistence lines calculated using the four-parameter non-ideal, non-symmetric approximation. The non-ideality parameters were obtained from a non-linear least square fit of the experimental data

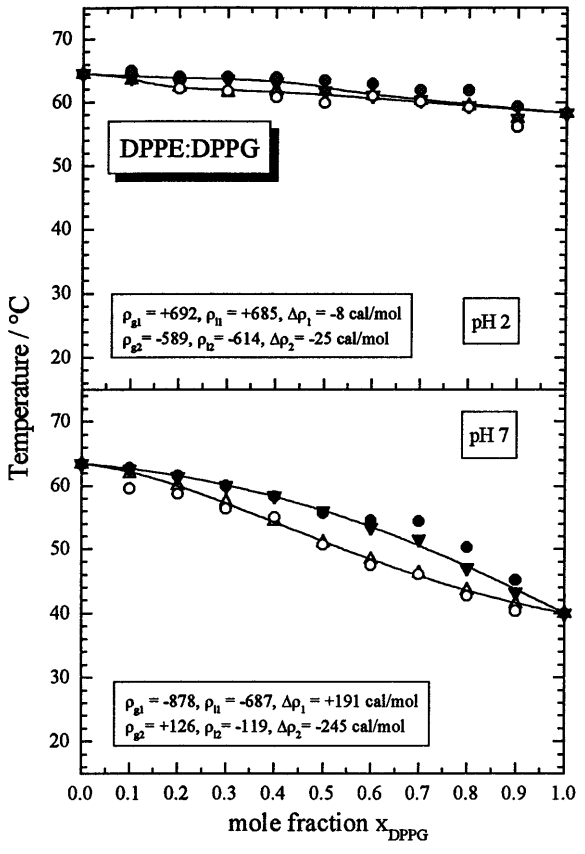

Fig. 6 Pseudobinary phase diagrams for the system DPPE:DPPG at pH 2 and pH 7. *Triangles* are $T(-)$ and $T(+)$ values obtained from the simulation of the C_p curve; *circles* are $T^{exp}(-)$ and $T^{exp}(+)$ values obtained by the usual empirical procedure. The *solid lines* are the coexistence lines calculated using the four-parameter non-ideal, non-symmetric approximation. The non-ideality parameters were obtained from a non-linear least square fit of the experimental data

very small for DMPE:DMPG whereas the corresponding data for the liquid-crystalline phase are $\rho_{l1} = +217$ cal/mol and $\rho_{l2} = -92$ cal/mol. As at pH 7, $\Delta\rho_1$ is again positive with +238 cal/mol; $\Delta\rho_2$ is negligible. For DPPE:DPPG mixtures, both non-ideality parameters ρ_1 are positive, but the terms ρ_1 are negative leading to a total $\Delta\rho$ of almost zero (see Fig. 9). The miscibility in the liquid-crystalline as well as the gel phase seems to be ideal.

DMPE:DPPG

pH 7. The T_m difference between the two components is only 8.8 °C. Both ρ_1 values are negative and $\Delta\rho$ is positive and decreases with increasing amounts of the PG component (Fig. 9). The mixing behavior is highly asymmetric for both phases (see Table 2). An upper azeotropic point seems to exist at $x_{DPPG} \approx 0.1$ (see Fig. 7).

pH 2. Protonation of DPPG shifts its phase transition temperature to 58 °C; it is now the higher melting component. From the thermograms at pH 2 (Fig. 3) it seems as if the onset temperature of melting is nearly constant up to a mole fraction of $x_{DPPG} = 0.5$. This implies a horizontal *solidus* line in this composition range with a miscibility gap. The system DMPE:DPPG at pH 2 shows positive ρ values, with $\rho_{g1,2} > \rho_{l1,2}$, which yield negative values for $\Delta\rho_1$ and $\Delta\rho_2$ (see Table 2). The shape of the phase diagram is complicated. Based on the temperature values $T(-)$ and $T(+)$ obtained from the simulation of the C_p curves, a phase diagram is obtained with a horizontal *solidus* line between x_{DPPG} of 0.55 and 0.9. Using empirically determined onset and end temperatures (T^{exp}) (open and solid circles in Fig. 7), a phase diagram with a similar shape (dotted lines in Fig. 7) is found. The two sets of non-ideality parameters obtained from the simulations are summarized in Table 3 and will be discussed later.

DPPE:DMPG

pH 7. This system shows the largest temperature difference for the main phase transition of the pure components ($\Delta T_m \approx 40$ °C, see Fig. 4). The simulation of the C_p

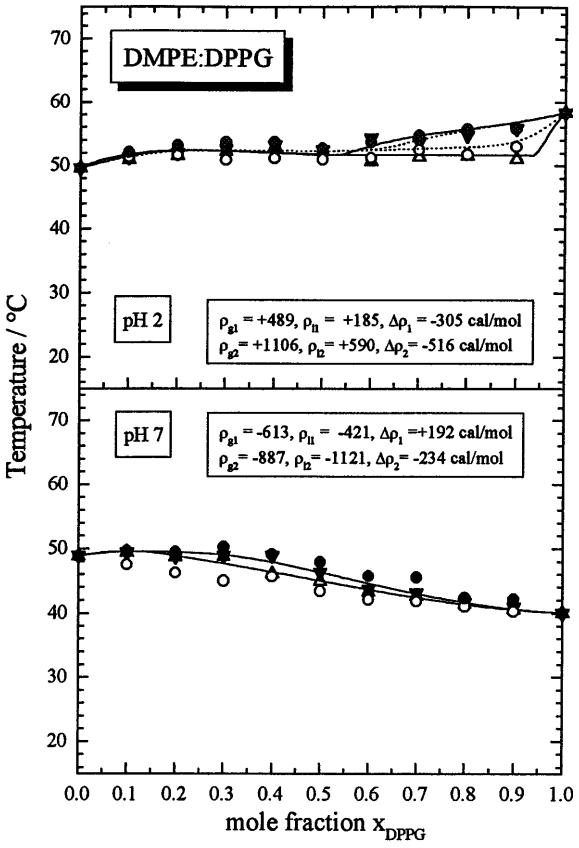

Fig. 7 Pseudobinary phase diagrams for the system DMPE:DPPG at pH 2 and pH. *Triangles* are $T(-)$ and $T(+)$ values obtained from the simulation of the C_p curve; *circles* are $T^{exp}(-)$ and $T^{exp}(+)$ values obtained by the usual empirical procedure. The *solid lines* are the coexistence lines calculated using the four-parameter non-ideal, non-symmetric approximation. The non-ideality parameters were obtained from a non-linear least square fit of the experimental data

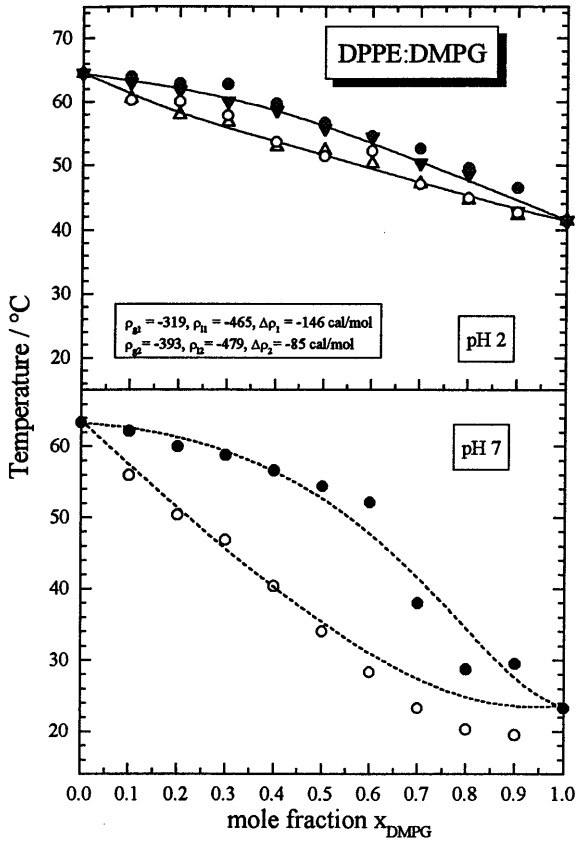

Fig. 8 Pseudobinary phase diagrams for the system DPPE:DMPG at pH 2 and pH 7. *Triangles* are $T(-)$ and $T(+)$ values obtained from the simulation of the C_p curve; *circles* are $T^{exp}(-)$ and $T^{exp}(+)$ values obtained by the usual empirical procedure. The *solid lines* for the system at pH 2 are the coexistence lines calculated using the four-parameter non-ideal, non-symmetric approximation. The non-ideality parameters were obtained from a non-linear least square fit of the experimental data. The phase diagram at pH 7 was not simulated; only the $T^{exp}(-)$ and $T^{exp}(+)$ values are shown (see text). The *dashed lines* are only included to guide the eye

curves was not successful for mixtures with less than 50 mol% of DPPE. The calorimetric curves and the temperatures for the onset and end of melting indicate a possible eutectic point at a DMPG mole fraction of 0.75–0.85, or a monotectic behavior in this region. The analysis is further complicated by the fact that the pretransition is shifted upwards with increasing DPPE content. We have refrained from simulating this phase diagram; the dashed lines in Fig. 8 were only drawn to guide the eye.

pH 2. At pH 2, the phase diagram indicates more or less ideal mixing (Fig. 8). All ρ values are negative and $\Delta\rho$ is also negative over the whole composition range and only marginally dependent on composition.

Discussion

We have focused our attention on the simulation of heat capacity curves of the main phase transition (gel to liquid-crystalline state), neglecting the pretransition. We have stated before that the simulation procedure is based on a two-state model for the transition and therefore a simplification of the real transition process. The justification to use this method despite its shortcomings was to remove some arbitrariness in the determination of the onset and end of "melting" temperatures which is inherent in the usual empirical procedures (Johann et al. 1996). The simulation of the DSC curves of the PE:PG mixtures yields fits which show that the underlying model for the transition is indeed too simple. The assumption of a temperature-independent broadening function is one of the reasons that no perfect fits can be achieved (Johann et al. 1996). Another reason is that the heat capacity curves were simulated assuming a symmetric, non-ideal mixing behavior for both phases, i.e. using only one non-ideality parameter for the ordered and for the liquid-crystalline phases, respectively. Finally, for pure phospholipids as well as for lipid mixtures, the transition involves a change in hydration of the headgroups. This is neglected in our model and also in all other transition models used so far (Lee 1977; Pink

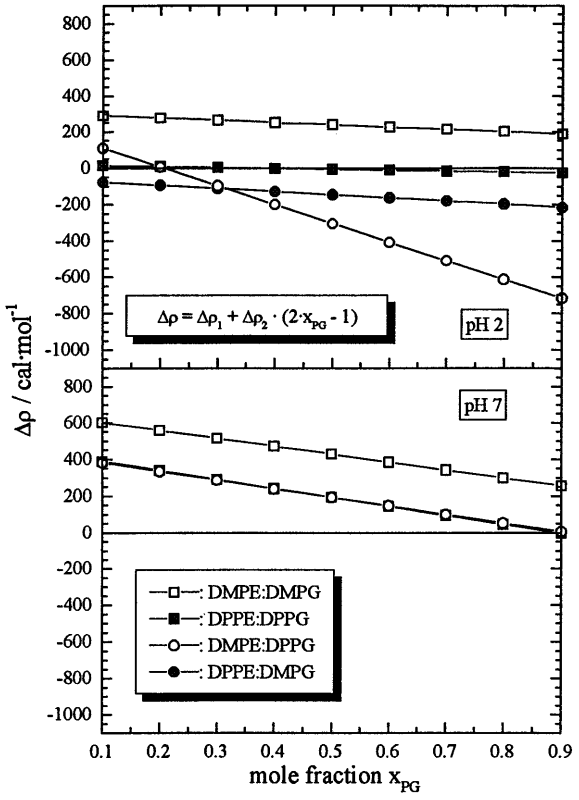

Fig. 9 Difference in non-ideality parameters $\Delta\rho_c = \Delta\rho_1 + \Delta\rho_2(2x_{PG}-1)$ for the PE:PG mixtures at pH 2 and pH 7. $\Delta\rho_1$ and $\Delta\rho_2$ are obtained from the simulation of the whole phase diagram

1990; Mouritsen 1991; Brumbaugh and Huang 1992; Heimburg and Marsh 1996; Mouritsen and Kinnunen 1996). The approach used here and by other groups for the analysis of lipid mixtures can therefore only be a first approximation without being able to quantitatively describe the thermodynamic behavior of these systems. Despite these shortcoming, the tendencies of mixing or demixing induced by varying the components or the pH can be analyzed with some confidence.

In general, the temperatures $T(-)$ and $T(+)$ obtained by the simulation of the heat capacity curves lead to narrower two-phase regions in the phase diagrams than those obtained by the usual empirical procedures (Johann et al. 1996). As a consequence, the absolute values of the non-ideality parameters are lower than those obtained by fitting the coexistence lines determined by the standard procedure. The general trends, however, are the same.

As observed before for other mixtures, the simulation of the heat capacity curves yield non-ideality parameters ρ which depend on the composition of the mixture, i.e. non-symmetric mixing behavior is observed.

Mixtures at pH 7

The tendency for the formation of a hydrogen bonding network between headgroups is particularly pronounced for PEs (Boggs 1987). At pH 7, the zwitterionic PE headgroup can act as donor (NH_3^+) as well as an acceptor for intermolecular hydrogen bonds (PO_2^-). The PG headgroup is negatively charged and can act as an hydrogen bond acceptor (PO_2^-). Also, the hydroxyl groups of the glycerol moiety can act as hydrogen bond donors, but their donor strength is weaker. The hydration properties of PG and PE are very different owing to these different hydrogen bonding capabilities and the additional hydroxyl groups in PGs. PEs are much less hydrated than PCs and PGs. The lamellar phases of the negatively charged PGs can swell indefinitely when no additional salt is present to shield the repulsive electrostatic interactions between opposing layers (Luzzati 1968; Ranck et al. 1974, 1977; McIntosh 1980; Wohlgemuth et al. 1980; Hauser et al. 1981, 1990; Blaurock 1982; Makowski and Li 1984; McIntosh and Simon 1986; Pascher et al. 1987, 1992). Because the PG headgroup occupies a much larger volume, the hydrocarbon chains of PG are tilted by ~30° ($L_{\beta'}$) relative to the normal of the plane of the bilayer, whereas PEs form an L_β phase with untilted chains (McIntosh 1980; Hauser et al. 1981).

The mixing properties of PE and PG in the gel phase should therefore be influenced by the difference in tilt angle of the hydrocarbon chains. From the different gel phase structure one would assume non-ideal mixing with a tendency for demixing of the two lipids. However, the introduction of PG in a PE bilayer facilitates the hydration of the PE headgroups (Tari and Huang 1989). The negative ρ_{g1} values observed are an indication of the

Table 2 Non-ideality parameters of mixing for PE:PG mixtures obtained from the simulation of the phase diagrams (the absolute values of the non-ideality parameters have relatively large errors of ca. ±200 cal mol^{-1}; the $\Delta\rho$ values are more precise). The DPPE:DMPG phase diagram at pH 7 was not simulated (see text)

System	ρ (cal mol^{-1})											
	pH 7						pH 2					
	ρ_{g1}	ρ_{l1}	ρ_{g2}	ρ_{l2}	$\Delta\rho_1$	$\Delta\rho_2$	ρ_{g1}	ρ_{l1}	ρ_{g2}	ρ_{l2}	$\Delta\rho_1$	$\Delta\rho_2$
DMPE:DMPG	−806	−379	−105	−322	+427	−218	−22	+217	−28	−92	+238	−63
DPPE:DPPG	−878	−687	+126	−119	+191	−245	+692	+685	−589	−614	−8	−25
DMPE:DPPG	−613	−421	−887	−1121	+192	−234	+489	+185	+1106	+590	−305	−516
DPPE:DMPG	–	–	–	–	–	–	−319	−465	−393	−479	−146	−85

Table 3 Non-ideality parameters obtained from the simulation of the phase diagram for the system DMPE:DPPG (0.1 M NaCl) at pH 2 using different sets of temperature data (see text)

ρ (cal mol^{-1})	ρ_{g1}	ρ_{l1}	ρ_{g2}	ρ_{l2}	$\Delta\rho_1$	$\Delta\rho_2$
ρ^{sim}	+489	+185	+1106	+590	−305	−516
ρ^{exp}	+310	+59	+852	+455	−251	−397

formation of mixed pairs. This is in contrast to the expectations based on the gel phase structure of the pure components.

For the L_α phase, the corresponding term ρ_{l1} is still negative, but the absolute values are smaller than for the gel phase. In the fluid phase, both lipids have disordered chains and the influence of the packing mismatch between chains and headgroup is reduced. A decrease in non-ideality of mixing is therefore to be expected and indeed observed. Apparently, the preferential formation of mixed pairs of PE-PG molecules in the ordered lamellar phase can be attributed to the ability of PGs to increase the hydration of the bilayer by disrupting the PE-PE contacts (Tari and Huang 1989). This leads to the formation of a mixed lipid pair composed of a "better hydrated" lipid (PG) with a lipid which is normally "less hydrated" (PE) (McIntosh and Simon 1986). This effect of PG plays a more important role for the gel phase, whereas for the liquid-crystalline phase the headgroups are more hydrated to begin with owing to the lateral expansion of the bilayers. Consequently, in nearly all cases $\rho_{g1} < \rho_{l1}$ (<0) is observed, which leads to a positive value for $\Delta\rho_1$. For the system DPPE:DMPG the non-ideality parameters are not reliable and cannot be discussed owing to the possibility of eutectic or monotectic behavior at low DPPE content.

The comparison of the systems DMPE:DMPG and DPPE:DPPG shows that the non-ideality parameters for the gel phase ρ_{g1} are similar with a value of $\sim$−840 cal/mol. However, slightly different ρ values were obtained for the liquid-crystalline phase, the shorter chain analogues showing less non-ideal mixing.

Mixtures at pH 2

Lowering the pH changes the phase structure of PG owing to protonation of the headgroup. Using X-ray diffraction, Watts et al. (1981) have shown that for negatively charged DPPG in the gel state (20 °C) the hydrocarbon chains have a tilt angle of 30° relative to the bilayer normal, whereas in the protonated state at pH 1–2 the tilt angle is less than 5°. For the liquid-crystalline state, the fluidity was found to be greater when the PG molecules are charged, owing to increased electrostatic repulsion. The fluidity was reduced when the PG headgroups are in the protonated state (Watts et al. 1978). Furthermore, protonation of PG induces the formation of a hydrogen bonding network between the phosphate groups (Tuchtenhagen 1994) which has also an effect on the mobility of PG in the bilayer and on the extent of hydration of the PG headgroup.

The shape of the phase diagrams having the same hydrocarbon chains for both lipids are very similar (see Figs. 5 and 6). Introduction of a difference in chain lengths between the two components leads to totally different phase diagrams, namely the DPPE:DMPG system shows a lens-like shape whereas DMPE:DPPG shows immiscibility in the gel phase at pH 2. Protonation of the PGs reduces the electrostatic repulsion between the PG headgroups in the layer and the hydration of the hydrophilic part is reduced (Hoekstra 1982; Tuchtenhagen 1994). Furthermore, the formation of a hydrogen bonding network between the phosphate groups is possible (Eibl and Woolley 1979). Therefore, the PG and PE headgroups become more similar in their behavior. The driving force for the formation of lipid mixed pairs, owing to an increase of hydration of the bilayer and particularly the PE component, is consequently distinctly reduced at pH 2 and the tendency for more positive non-ideality parameters (less negative ρ compared to the systems at pH 7) indicates that the lipids prefer the formation of like pairs.

From the analysis of the phase diagrams of the PE:PG systems at pH 2, the following trend can be observed. The non-ideality parameters ρ_g obtained from the simulation of the phase diagrams become less negative or even positive compared to the systems at neutral pH, i.e. in all cases ρ_{g1}(pH 7) $<$ ρ_{g1}(pH 2). This effect is also observed for ρ_{l1}. In addition, $\Delta\rho$ is reduced for the systems at pH 2 compared to systems at pH 7.

The analysis of the phase diagram of DMPE:DPPG at pH 2 is more complicated. The horizontal solidus line between x_{DPPG} = 0.55–0.9 is an indication of a miscibility gap in the gel phase. This is indicated by strongly positive ρ_{g1} and ρ_{g2} values (see Table 2). We have also calculated this phase diagram using temperature data obtained by the usual empirical procedure (Table 3). These non-ideality parameters (ρ^{exp}) show similar behavior as the non-ideality parameter obtained from the $T(-)$ and $T(+)$ values (ρ^{sim}). The reason for the complicated mixing behavior of this system is not clear.

Comparison with PC:PG mixtures and the influence of protonation on the mixing behavior

An analogous investigation of the miscibility in PC:PG systems with the same chain length differences was performed previously (Garidel et al. 1997b). Like PEs, PCs have a zwitterionic headgroup, but have larger hydration numbers and a phase behavior similar to PGs.

In the PE:PG systems, protonation of PG leads to an increase of the non-ideality parameter ρ_1:$\rho_{g,l1}$(pH 7) $<$ $\rho_{g,l1}$(pH 2), with $\rho_{g,l1}$(pH 7) $<$ 0. Also, the $\Delta\rho$ values, which are positive at pH 7, decrease upon protonation of the PG component (Fig. 9). In PC:PG systems at

pH 7, the $\Delta\rho$ values are mostly negative or close to zero and become more positive upon protonation of the PG component. This behavior obviously reflects a combination of several effects, namely changes in headgroup charge with concomitant hydration changes and changes in tilt angle of the chains in the gel phase. Protonation of PG in mixtures with PE reduces the differences in hydration and phase behavior of the two components, whereas in mixtures of PG with PC the opposite is true. Therefore, in the first case the non-ideal mixing behavior is decreased, and the previously favored formation of mixed PE:PG pairs at pH 7 is reduced when PG is protonated. In PC:PG mixtures the non-ideal mixing behavior is increased upon protonation of PG. In the system DPPC:DMPG at pH 2, even an upper azeotropic point occurs in the phase diagram and ρ_{l1} is positive and has an extremely large value (Garidel et al. 1997b), whereas for the corresponding mixture with PE (DPPE:DMPG at pH 2) a lens-like phase diagram with a negative ρ_{l1} is observed.

Summary and conclusions

The mixing behavior of PE:PG mixtures was studied at different degrees of ionization of the PG component and for different acyl chain lengths of the lipids using DSC. The miscibility in PE:PG mixtures strongly depends on pH, i.e. the degree of ionization of the PG component. The non-ideality parameters obtained from the simulation of the phase diagrams show that, at pH 7, mixed PE:PG pairing is favored, particularly for the gel phase. This can be explained by changes in hydration of the headgroup region of the bilayer induced by the PG component in the mixture. Protonation of the PG headroups leads to an increase of ρ_{g1} and ρ_{l1}, so that in all cases $\rho_{g,l1}$(pH 7) < $\rho_{g,l1}$(pH 2). This can be interpreted as a protonation induced destabilization of the mixed pairs, i.e. the mixtures become more ideal when the PG headgroup is protonated. This is in contrast to the behavior of PC:PG mixtures, where the opposite effect was observed.

The observation of increased hydration of the PE headgroups when PGs are incorporated could be of benefit for bacterial membranes. Incorporation of PGs not only introduces a net negative charge to the bilayers but also leads to the formation of PE:PG mixed pairs. This process prevents the formation of phase boundaries caused by demixing of lipids in the bilayer plane, which could lead to an increase in membrane permeability and a decrease in membrane stability.

Acknowledgements We thank L. Mennicke for supplying us with the simulation programs for the C_p curves and C. Johann for intensive and helpful discussions. Furthermore, we thank A. Müller and N. Papke for their technical participation in these studies. This work was supported by grants from the Deutsche Forschungsgemeinschaft (Bl 182/7-3) and the Fonds der Chemischen Industrie.

References

Blaurock AF (1982) Evidence of bilayer structure and of membrane interactions from X-ray diffraction analysis. Biochim Biophys Acta 650: 167–207

Bloom M, Evans E, Mouritsen OG (1991) Physical properties of the fluid lipid-bilayer component of cell membranes: a perspective. Q Rev Biophys 24: 293–397

Blume A (1988) Applications of calorimetry to lipid model membranes. In: Hidalgo C (ed) Physical properties of biological membranes and their function implications. Plenum Press, New York, pp 71–121

Blume A (1991) Biological calorimetry: membranes. Thermochim Acta 193: .299–347

Boggs JM (1987) Lipid intermolecular hydrogen bonding: influence on structural organisation and membrane function. Biochim Biophys Acta 906: 353–404

Borle F, Seelig J (1985) Structure of *Escherichia coli* membranes. Deuterium magnetic resonance studies of the phosphoglycerol head group in intact cells and model membranes. Biochemistry 22: 5536–5544

Brumbaugh EE, Huang C (1992) Parameter estimation in binary mixtures of phospholipids. Methods Enzymol 210: 521–539

Cevc G (1990) Membrane electrostatics. Biochim Biophys Acta 1031–1033: 311–382

Cevc G, Watts A, Marsh D (1980) Non-electrostatic contribution to the titration of the ordered-fluid phase transition of phosphatidylglycerol bilayers. FEBS Lett 120: 267–270

Cronan JE, Gelman EP (1975) Physical properties of membrane lipids: biological relevance and regulation. Bacteriol Rev 39: 232–256

Cronan JE Jr, Vagelos RR (1972) Metabolism and function of the membrane phospholipids of *Escherichia coli*. Biochim Biophys Acta 265: 25–60

Denisov G, Wanaski S, Luan P, Glaser M, McLaughlin S (1998) Binding of basic peptides to membranes produces lateral domains enriched in the acidic lipids phosphatidylserine and phosphatidylinositol 4,5-bisphosphate: an electrostatic model and experimental results. Biophys J 74: 731–744

Eibl H, Woolley P (1979) Electrostatic interactions at charged lipid membranes. Hydrogen bonds in lipid membrane surface. Biophys Chem 10: 261–271

Gally HU, Pluschke G, Overath P, Seelig J (1980) Structure of *Escherichia coli* membranes. Fatty acyl chain order parameter of inner and outer membranes and derived liposomes. Biochemistry 19: 1638–1643

Garidel P, Johann C, Blume A (1997a) Nonideal mixing and phase separation in phosphatidylcholine-phosphatidic acid mixtures as a function of acyl chain length and pH. Biophys J 72: 2196–2210

Garidel P, Johann C, Mennicke L, Blume A (1997b) The mixing behaviour of pseudobinary phosphatidylcholine-phosphatidylglycerol mixtures as a function of pH and acyl chain length. Eur Biophys J 26: 447–459

Hauser H, Pascher I, Pearson RH, Sundell S (1981) Preferred conformation and molecular packing of phosphatidylethanolamine and phosphatidylcholine. Biochim Biophys Acta 650: 21–51

Hauser H, Pascher I, Sundell S (1990) Preferred conformation of the diacylglycerol moiety of phospholipids. In: Brasseur R (ed) Molecular description of biological membranes by computer aided conformational analysis, vol I, chap 1B2. CRC Press, Boca Raton, pp 267–285

Heimburg T, Marsh D (1996) Thermodynamics of the interaction of proteins with lipid membranes. In: Merz KM Jr, Roux B (eds) Biological membranes. A molecular perspective from computation and experiment. Birkhäuser, Boston, pp 405–462

Hoekstra D (1982) Role of lipid phase separations and membrane hydration in phospholipid vesicle fusion. Biochemistry 21: 2833–2840

Jacobson K, Papahadjopoulos D (1975) Phase transitions and separations in phospholipid membranes induced by changes in temperature, pH, and concentration of bivalent cations. Biochemistry 14: 152–161

Johann C, Garidel P, Mennicke L, Blume A (1996) New approaches for the simulation of heat capacity curves and phase diagrams of pseudobinary phospholipid mixtures. Biophys J 71: 3215–3228

Lee AG (1977) Lipid phase transitions and phase diagrams. II. Mixtures involving lipids. Biochim Biophys Acta 472: 285–344

Luzzati V (1968) X-ray diffraction studies of lipid-water systems. Biol Membr 1: 71–123

Mabrey S, Sturtevant JM (1976) Investigation of phase transition of lipids and lipid mixtures by high sensitivity differential scanning calorimetry. Proc Natl Acad Sci USA 73: 3862–3866

MacFarlane MG (1964) Phosphatidylglycerols and lipoamino acids. Adv Lipid Res 2: 91–125

Makowski L, Li J (1984) X-ray diffraction and electron microscope studies of the molecular structure of biological membranes. In: Chapman D (ed) Biomembrane, structure and function. (Topics in molecular and structural biology 4) Verlag Chemie, Weinheim, pp 43–166

McIntosh TJ (1980) Differences in hydrocarbon chain tilt between hydrated phosphatidylethanolamine and phosphatidylcholine bilayers. Biophys J 29: 237–246

McIntosh TJ, Simon SA (1986) Area per molecule and distribution of water in fully hydrated dilauroylphosphatidylethanolamine bilayers. Biochemistry 25: 4948–4952

Mennicke L (1995) Die Simulation der Wärmekapazitätskurven und die Berechnung der Phasendiagramme von pseudobinären Lipid-Lipid-Wasser Systemen am Beispiel von gemischtkettigen Phospholipiden mit verzweigten Acylketten. PhD thesis, University of Kaiserslautern, Germany

Metcalf TN, Wang JL, Schindler M (1986) Lateral diffusion of phospholipids in the plasma membrane of soybean protoplasts: evidence for membrane lipid domains. Proc Natl Acad Sci USA 83: 95–99

Mouritsen OG (1991) Theoretical models of phospholipid phase transitions. Chem Phys Lipids 57: 179–194

Mouritsen OG, Kinnunen PKJ (1996) Role of lipid organization and dynamics in membrane functionality. In: Merz KM Jr, Roux B (eds) Biological membranes. A molecular perspective from computation and experiment. Birkhäuser, Boston, pp 463–502

Pascher I, Sundell S, Harlos K, Eibl H (1987) Conformation and packing properties of membrane lipids: the crystal structure of sodium dimyristoylphosphatidylglycerol. Biochim Biophys Acta 896: 77–88

Pascher I, Lundmark M, Nyholm P-G and Sundell S (1992) Crystal structures of membrane lipids. Biochim Biophys Acta 1113: 339–373

Pink D (1990) Computer simulations of biological membranes. In: Brasseur R (ed) Molecular description of biological membrane components by computer aided conformational analysis. CRC Press, Boca Raton, pp 151–170

Ranck JL, Mateu L, Sadler DM, Tardieu A, Gulik-Krzywicki T, Luzzati V (1974) Order-disorder conformational transitions of the hydrocarbon chains of lipids. J Mol Biol 85: 249–277

Ranck JL, Keira T, Luzzati V (1977) A novel packing of the hydrocarbon chains in lipids. The low temperature phases of dipalmitoylphosphatidylglycerol. Biochim Biophys Acta 488: 432–441

Silvius JR, Gagné J (1984a) Lipid phase behaviour and calcium induced fusion of phosphatidylethanolamine-phosphatidylserine vesicles. Calorimetric and fusion studies. Biochemistry 23: 3232–4340

Silvius JR, Gagné J (1984b) Calcium-induced fusion and lateral phase separation in phosphatidylcholine-phosphatidylserine vesicles. Correlation by calorimetric and fusion measurements. Biochemistry 23: 3241–4347

Standish MM, Pethica BA (1968) Surface pressure and surface potential study of a synthetic phospholipid at the air/water interface. Trans Faraday Soc 64: 1113–1122

Tari A, Huang L (1989) Structure and function relationship of phosphatidylglycerol in the stabilisation of the phosphatidylethanolamine bilayer. Biochemistry 28: 7708–7712

Tatulian SA (1992) Ionisation and ion binding. In: Cevc G (ed) Phospholipids handbook, Chap. 14. Dekker, New York, pp 511–552

Tocanne J-F, Cézanne L, Lopez A, Piknova B, Schram V, Tournier J-F, Welby M (1994) Lipid domains and lipid/protein interactions in biological membranes. Chem Phys Lipids 73: 139–158

Träuble H (1976) Membrane electrostatics. In: Abrahamsson S, Pascher I (eds) Structure of biological membranes. Plenum Press, New York, pp 509–550

Träuble H, Eibl HJ (1974) Electrostatic effects on lipid phase transitions: membrane structure and ionic environment. Proc Natl Acad Sci USA 71: 214–221

Träuble H, Teubner M, Woolley P, Eibl H (1976) Electrostatic interactions at charged lipid membranes. 1. Effects of pH and univalent cations on membrane structure. Biophys Chem 4: 319–342

Tuchtenhagen J (1994) Kalorimetrische und FT-IR-spektroskopische Untersuchungen an Phospholipidmodellmembranen. PhD thesis, University of Kaiserslautern, Germany

Vaz WLC (1994) Diffusion and reaction in phase-separated membranes. Biophys Chem 50: 139–145

Vaz WLC (1995) Percolation properties of two-component, two-phase phospholipid bilayers. Mol Membr Biol 12: 39–43

Watts A, Harlos K, Maschke W, Marsh D (1978) Control of the structure and fluidity of phosphatidylglycerol bilayers by pH titration. Biochim Biophys Acta 510: 63–74

Watts A, Harlos K, Marsh D (1981) Charge induced tilt in ordered phase phosphatidylglycerol bilayers. Evidence from X-ray diffraction. Biochim Biophys Acta 645: 91–96

Welti R, Glaser M (1994) Lipid domains in model and biological membranes. Chem Phys Lipids 73: 121–137

Wohlgemuth R, Waespe-Sarvcevc N, Seelig J (1980) Bilayers of phosphatidylglycerol. A deuterium and phosphorus nuclear magnetic resonance study of the head-group-region. Biochemistry 19: 3315–3321

Yang L, Glaser M (1996) Formation of membrane domains during the activation of protein kinase C. Biochemistry 35: 13966–13974